

Three-flavour neutrino oscillation update

Thomas Schwetz^{1,4}, Mariam Tórtola² and José W F Valle³

¹ Theory Division, Physics Department, CERN, CH-1211 Geneva 23, Switzerland

² Departamento de Física and CFTP, Instituto Superior Técnico, Av. Rovisco Pais 1, 1049-001 Lisboa, Portugal

³ AHEP Group, Instituto de Física Corpuscular—CSIC/Universitat de València, Edificio Institutos de Paterna, Apt 22085, E-46071 Valencia, Spain
E-mail: schwetz@cern.ch, mariam@cftp.ist.utl.pt and valle@ific.uv.es

New Journal of Physics **10** (2008) 113011 (10pp)

Received 19 August 2008

Published 10 November 2008

Online at <http://www.njp.org/>

doi:10.1088/1367-2630/10/11/113011

Abstract. We review the present status of three-flavour neutrino oscillations, taking into account the latest available neutrino oscillation data presented at the Neutrino 2008 Conference. This includes the data released this summer by the MINOS collaboration, the data of the neutral current counter phase of the Sudbury Neutrino Observatory (SNO) solar neutrino experiment, as well as the latest KamLAND and Borexino data. We give the updated determinations of the leading ‘solar’ and ‘atmospheric’ oscillation parameters. We find from global data that the mixing angle θ_{13} is consistent with zero within 0.9σ and we derive an upper bound of $\sin^2\theta_{13} \leq 0.035$ (0.056) at 90% confidence level (CL) (3σ).

Contents

1. Introduction	2
2. The leading ‘solar’ and ‘atmospheric’ oscillation parameters	2
3. Status of θ_{13}	6
4. Summary	8
Acknowledgments	9
References	9

⁴ Author to whom any correspondence should be addressed.

1. Introduction

Thanks to the synergy among a variety of experiments involving solar and atmospheric neutrinos, as well as man-made neutrinos at nuclear power plants and accelerators (for recent reviews, see [1]), neutrino physics has undergone a revolution over the last decade or so. The long-sought-for phenomenon of neutrino oscillations has been finally established, demonstrating that neutrino flavour states (ν_e, ν_μ, ν_τ) are indeed quantum superpositions of states (ν_1, ν_2, ν_3) with definite masses m_i [2]. The simplest unitary form of the lepton mixing matrix relating flavour and mass eigenstate neutrinos is given in terms of three mixing angles ($\theta_{12}, \theta_{13}, \theta_{23}$) and three CP-violating phases, only one of which affects (conventional) neutrino oscillations [3]. Here, we consider only the effect of the mixing angles in current oscillation experiments; the sensitivity to CP violation effects remains an open challenge for future experiments [4, 5]. Together with the mass splitting parameters $\Delta m_{21}^2 \equiv m_2^2 - m_1^2$ and $\Delta m_{31}^2 \equiv m_3^2 - m_1^2$, the angles θ_{12}, θ_{23} are rather well determined by the oscillation data. In contrast, so far only upper bounds can be placed upon θ_{13} , mainly following from the null results of the short-baseline CHOOZ reactor experiment [6] with some effect also from solar and KamLAND data, especially at low Δm_{31}^2 values [7].

Here, we present an update on the three-flavour oscillation analyses of [7, 8]. This new analysis includes the data released this summer by the Main Injector Neutrino Oscillation Search (MINOS) collaboration [9], the data from the neutral current (NC) counter phase of the Sudbury Neutrino Observatory (SNO) experiment (SNO neutral current detectors) [10], the latest KamLAND [11] and Borexino [12] data, as well as the results of a recent re-analysis of the Gallex/GNO solar neutrino data presented at the Neutrino 2008 Conference [13]. In section 2, we discuss the status of the parameters relevant for the leading oscillation modes in solar and atmospheric neutrinos. In section 3, we present the updated limits on θ_{13} and discuss the recent claims for possible hints in favour of a nonzero value made in [14]–[16]. We summarize in section 4.

2. The leading ‘solar’ and ‘atmospheric’ oscillation parameters

Let us first discuss the status of the solar parameters θ_{12} and Δm_{21}^2 . The latest data released from the KamLAND reactor experiment [11] have increased the exposure almost fourfold over previous results [17] to 2.44×10^{32} proton \times year due to longer lifetime and an enlarged fiducial volume, corresponding to a total exposure of 2881 tonne \times year. Apart from the increased statistics, also systematic uncertainties have been improved: thanks to the full volume calibration the error on the fiducial mass has been reduced from 4.7 to 1.8%. Details of our KamLAND analysis are described in appendix A of [8]. We use the data binned in equal bins in $1/E$ to make optimal use of spectral information; we take into account the (small) matter effect and carefully include various systematics following Huber and Schwetz [18]. As previously, we restrict the analysis to the prompt energy range above 2.6 MeV where the contributions from geo-neutrinos [19] as well as backgrounds are small and the selection efficiency is roughly constant [11]. In that energy range, 1549 reactor neutrino events and a background of 63 events are expected without oscillations, whereas the observed number of events is 985 [20].

The SNO has released the data on its last phase, where the neutrons produced in the neutrino NC interaction with deuterium are detected mainly by an array of ^3He proportional counters to measure the rate of NC interactions in heavy water and precisely determine

the total active boron solar neutrino flux, yielding the result $5.54_{-0.31}^{+0.33}(\text{stat})_{-0.34}^{+0.36}(\text{syst}) \times 10^6 \text{ cm}^{-2} \text{ s}^{-1}$ [10]. The independent ^3He neutral current detectors (NCD) provide a measurement of the neutral current flux uncorrelated with the charged current rate from solar ν_e , different from the statistical CC/NC separation of previous SNO phases. Since the total NC rate receives contributions from the NCD as well as from the photo multiplier tubes (PMTs) (as previously), a small (anti-) correlation between CC and NC remains. Following Fogli *et al* [16], we assume a correlation of $\rho = -0.15$. In our SNO analysis, we add the new data on the CC and NC fluxes to the previous results [21] assuming no correlation between the NCD phase and the previous salt phase, see [7] for further details. The main impact of the new SNO data is due to the lower value for the observed CC/NC ratio, $(\phi_{\text{CC}}/\phi_{\text{NC}})^{\text{NCD}} = 0.301 \pm 0.033$ [10], compared with the previous value $(\phi_{\text{CC}}/\phi_{\text{NC}})^{\text{salt}} = 0.34 \pm 0.038$ [21]. Since for ^8B neutrinos $\phi_{\text{CC}}/\phi_{\text{NC}} \approx P_{ee} \approx \sin^2\theta_{12}$, adding the new data point on this ratio with the lower value leads to a stronger upper bound on $\sin^2\theta_{12}$.

We also include the direct measurement of the ^7Be solar neutrino signal rate performed by the Borexino collaboration [12]. They report an interaction rate of the 0.862 MeV ^7Be neutrinos of $49 \pm 3(\text{stat}) \pm 4(\text{syst})$ counts (day 100 tonnes) $^{-1}$. This measurement constitutes the first direct determination of the survival probability for solar ν_e in the transition region between matter-enhanced and vacuum-driven oscillations. The survival probability of 0.862 MeV ^7Be neutrinos is determined to be $P_{ee}^{7\text{Be,obs}} = 0.56 \pm 0.1$. We find that with the present errors, Borexino plays no significant role in the determination of neutrino oscillation parameters. Apart from the fact that the uncertainty on the survival probability is about a factor 3 larger than e.g. the uncertainty on the SNO CC/NC ratio measurement, it turns out that the observed value for P_{ee} quoted above practically coincides (within 0.1σ) with the prediction at the best fit point: $P_{ee}^{7\text{Be,pred}} = 0.55$.

The new data from SNO and Borexino are combined with the global data on solar neutrinos [22]–[25], where we take into account the results of a recent re-analysis of the Gallex data yielding a combined Gallex and GNO rate of $67.6 \pm 4.0 \pm 3.2$ solar neutrino units (SNU) [13].

Figure 1 illustrates how the determination of the leading solar oscillation parameters θ_{12} and Δm_{21}^2 emerges from the complementarity of solar and reactor neutrinos. From the global three-flavour analysis, we find (1σ errors)

$$\sin^2\theta_{12} = 0.304_{-0.016}^{+0.022}, \quad \Delta m_{21}^2 = 7.65_{-0.20}^{+0.23} \times 10^{-5} \text{ eV}^2. \quad (1)$$

The numerical χ^2 profiles shown in figure 1 have to very good accuracy the Gaussian shape $\chi^2 = (x - x_{\text{best}})^2/\sigma^2$, when the different σ for upper and lower branches are used as given in equation (1). Spectral information from KamLAND data leads to an accurate determination of Δm_{21}^2 with the remarkable precision of 8% at 3σ , defined as $(x^{\text{upper}} - x^{\text{lower}})/(x^{\text{upper}} + x^{\text{lower}})$. We find that the main limitation for the Δm_{21}^2 measurement comes from the uncertainty on the energy scale in KamLAND of 1.5%. KamLAND data start also to contribute to the lower bound on $\sin^2\theta_{12}$, whereas the upper bound is dominated by solar data, most importantly by the CC/NC solar neutrino rate measured by SNO. The SNO-NCD measurement reduces the 3σ upper bound on $\sin^2\theta_{12}$ from 0.40 [8] to 0.37.

Let us now move to a discussion of the status of the leading atmospheric parameters θ_{23} and Δm_{31}^2 . The MINOS experiment has reported new results on ν_μ disappearance with a baseline of 735 km based on a 2-year exposure from the Fermilab NuMI beam. Its data, recorded between May 2005 and July 2007, correspond to a total of 3.36×10^{20} protons on target (POT) [9], more

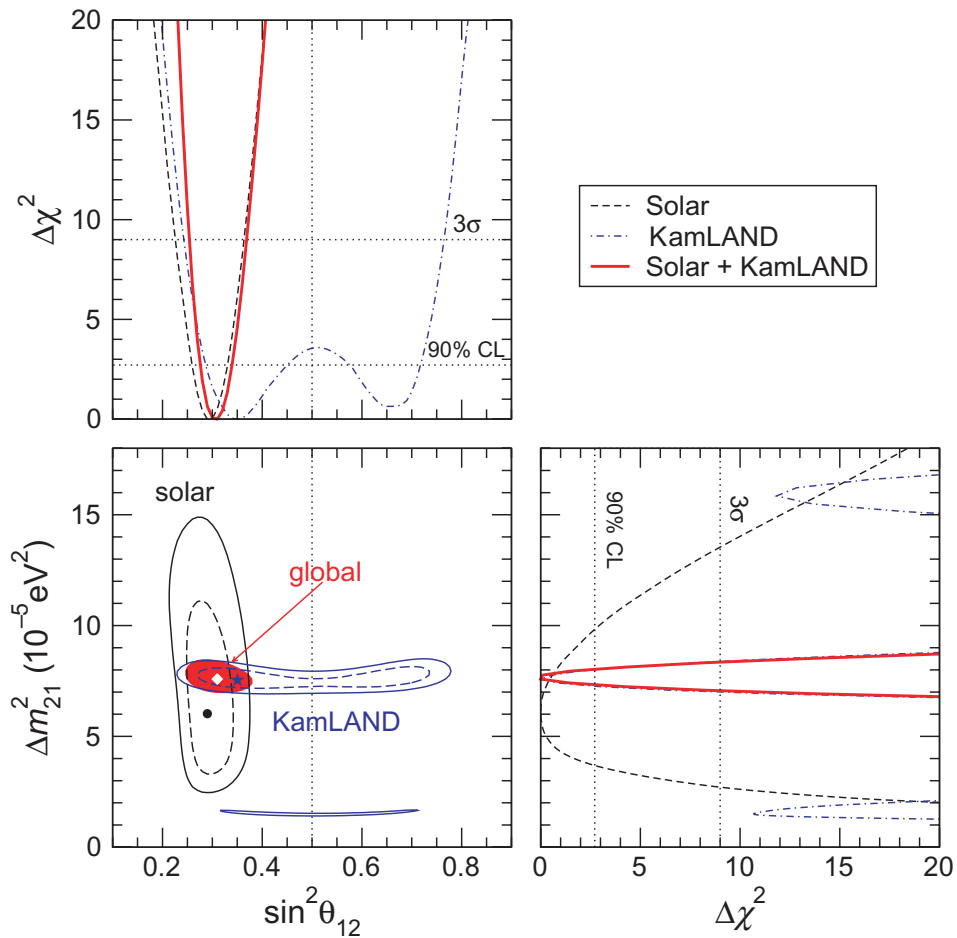


Figure 1. Determination of the leading ‘solar’ oscillation parameters from the interplay of data from artificial and natural neutrino sources. We show χ^2 -profiles and allowed regions at 90 and 99.73% confidence level (CL) (2 degrees of freedom (d.o.f.)) for solar and KamLAND, as well as the 99.73% CL region for the combined analysis. The dot, star and diamond indicate the best fit points of solar data, KamLAND and global data, respectively. We minimize with respect to Δm_{31}^2 , θ_{23} and θ_{13} , including always atmospheric, MINOS, K2K and CHOOZ data.

than doubling the POT with respect to MINOS run I [26], and increasing the exposure used in the latest version of [8] (in its arXiv version, the review [8] provides results updated as of September 2007) by about 34%. The latest data confirm the energy-dependent disappearance of ν_μ , showing significantly less events than expected in the case of no oscillations in the energy range $\lesssim 6$ GeV, whereas the high-energy part of the spectrum is consistent with the no oscillation expectation. We include this result in our analysis by fitting the event spectrum given in figure 2 of [9]. Current MINOS data largely supersede the pioneering K2K measurement [27] which by now gives only a very minor contribution to the Δm_{31}^2 measurement.

We combine the long-baseline accelerator data with atmospheric neutrino measurements from Super-Kamiokande [28], using the results of [8], see references cited therein for details.

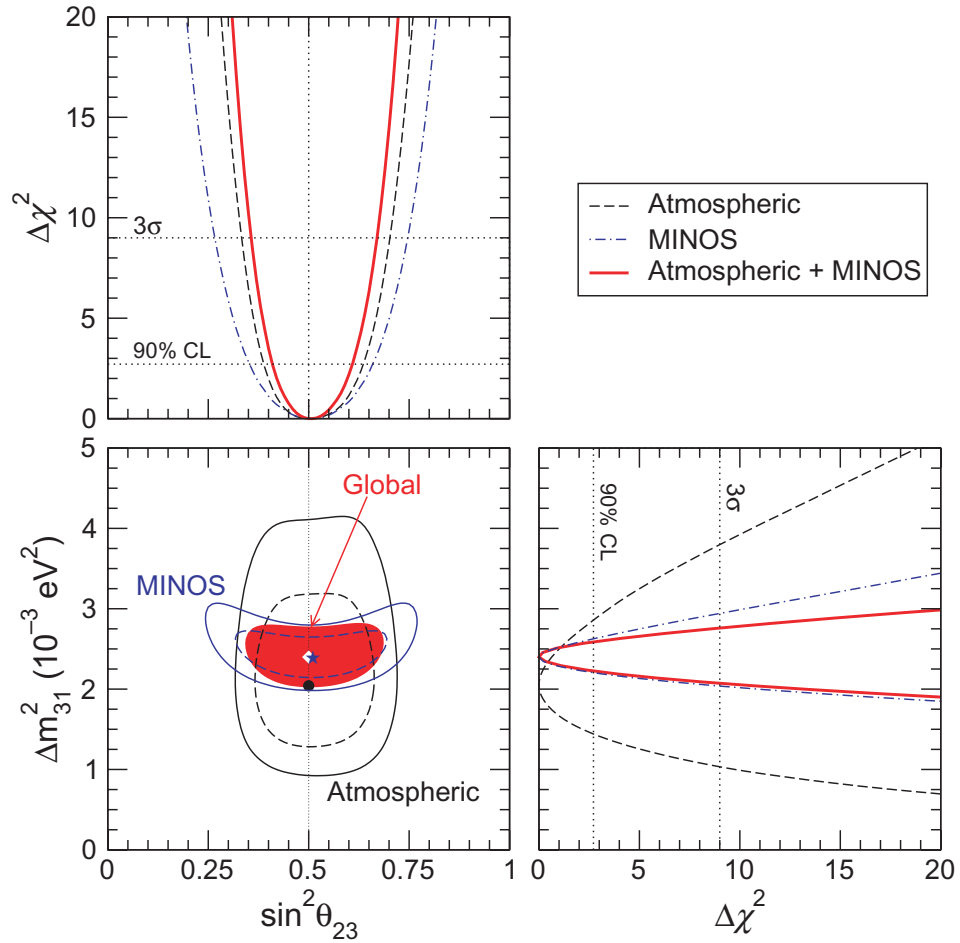


Figure 2. Determination of the leading ‘atmospheric’ oscillation parameters from the interplay of data from artificial and natural neutrino sources. We show χ^2 -profiles and allowed regions at 90 and 99.73% CL (2 d.o.f.) for atmospheric and MINOS, as well as the 99.73% CL region for the combined analysis (including also K2K). The dot, star and diamond indicate the best fit points of atmospheric data, MINOS and global data, respectively. We minimize with respect to Δm_{21}^2 , θ_{12} and θ_{13} , including always solar, KamLAND and CHOOZ data.

In this analysis, sub-leading effects of Δm_{21}^2 in atmospheric data are neglected, but effects of θ_{13} are included, in a similar spirit as in [29].

Figure 2 illustrates how the determination of the leading atmospheric oscillation parameters θ_{23} and $|\Delta m_{31}^2|$ emerges from the complementarity of atmospheric and accelerator neutrino data. We find the following best fit points and 1σ errors:

$$\sin^2\theta_{23} = 0.50_{-0.06}^{+0.07}, \quad |\Delta m_{31}^2| = 2.40_{-0.11}^{+0.12} \times 10^{-3} \text{ eV}^2. \quad (2)$$

The determination of $|\Delta m_{31}^2|$ is dominated by spectral data from the MINOS long-baseline ν_μ disappearance experiment, where the sign of Δm_{31}^2 (i.e. the neutrino mass hierarchy) is undetermined by the present data. The measurement of the mixing angle θ_{23} is still largely

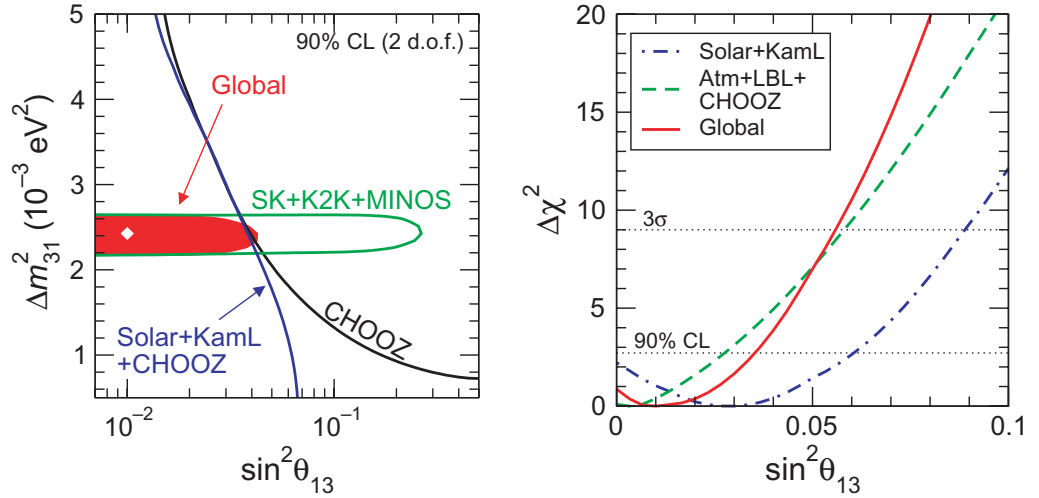


Figure 3. Constraints on $\sin^2 \theta_{13}$ from different parts of the global data.

dominated by atmospheric neutrino data from Super-Kamiokande with a best fit point at maximal mixing. Small deviations from maximal mixing due to sub-leading three-flavour effects have been found in [30, 31], see, however, also [32] for a preliminary analysis of Super-Kamiokande. A comparison of these subtle effects can be found in [33]. At present, deviations from maximality are not statistically significant.

3. Status of θ_{13}

The third mixing angle θ_{13} would characterize the magnitude of CP violation in neutrino oscillations. Together with the determination of the neutrino mass spectrum hierarchy (i.e. the sign of Δm^2_{31}) it constitutes a major open challenge for any future investigation of neutrino oscillations [4, 5].

Figure 3 summarizes the information on θ_{13} from the present data. Similar to the case of the leading oscillation parameters, also the bound on θ_{13} emerges from an interplay of different data sets, as illustrated in the left panel of figure 3. An important contribution to the bound comes, of course, from the CHOOZ reactor experiment [6] combined with the determination of $|\Delta m^2_{31}|$ from atmospheric and long-baseline experiments. Due to a complementarity of low- and high-energy solar neutrino data, as well as solar and KamLAND data, one finds that also solar + KamLAND provide a nontrivial constraint on θ_{13} , see e.g. [7, 8, 34]. We obtain at 90% CL (3σ) the following limits⁵:

$$\sin^2 \theta_{13} \leq \begin{cases} 0.060(0.089) & (\text{solar} + \text{KamLAND}), \\ 0.027(0.058) & (\text{CHOOZ} + \text{atm} + \text{K2K} + \text{MINOS}), \\ 0.035(0.056) & (\text{global data}). \end{cases} \quad (3)$$

In the global analysis, we find a slight weakening of the upper bound on $\sin^2 \theta_{13}$ due to the new data from 0.04 (see [33] or v5 of [8]) to 0.056 at 3σ . The reason for this is twofold.

⁵ Note that the bounds given in equation (3) are obtained for 1 d.o.f., whereas in figure 3 (left) the 90% CL regions for 2 d.o.f. are shown.

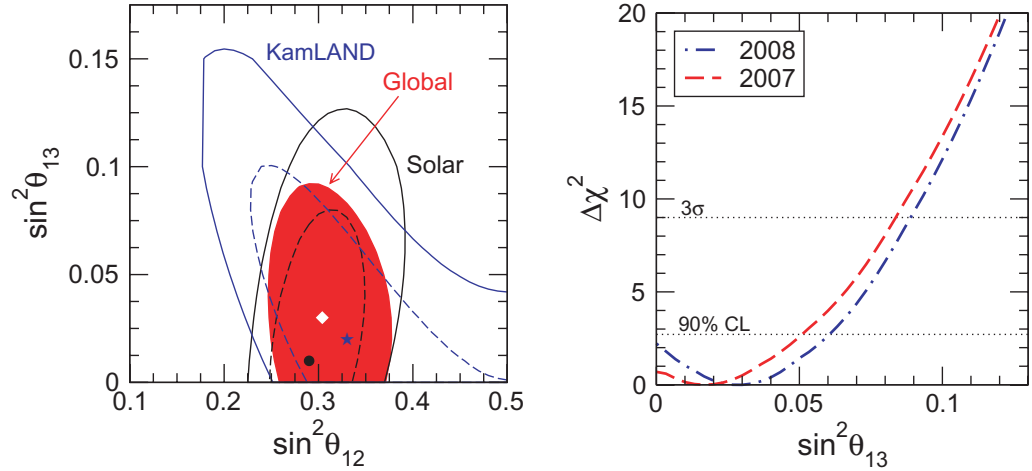


Figure 4. Left: allowed regions in the $(\theta_{12} - \theta_{13})$ plane at 90 and 99.73% CL (2 d.o.f.) for solar and KamLAND, as well as the 99.73% CL region for the combined analysis. Δm_{21}^2 is fixed at its best fit point. The dot, star and diamond indicate the best fit points of solar, KamLAND and combined data, respectively. Right: χ^2 profile from solar and KamLAND data with and without the 2008 SNO-NCD data.

Firstly, the shift of the allowed range for $|\Delta m_{31}^2|$ to lower values due to the new MINOS data implies a slightly weaker constraint on $\sin^2 \theta_{13}$ (cf figure 3, left), and secondly, the combination of solar and new KamLAND data prefers a slightly nonzero value of $\sin^2 \theta_{13}$ which, though not statistically significant, also results in a weaker constraint in the global fit (cf figure 3, right).

As has been noted in [16], the slight downward shift of the SNO CC/NC ratio due to the SNO-NCD data leads to a ‘hint’ for a nonzero value of θ_{13} . From the combination of solar and KamLAND data, we find a best fit value of $\sin^2 \theta_{13} = 0.03$ with $\Delta\chi^2 = 2.2$ for $\theta_{13} = 0$, which corresponds to a 1.5σ effect (86% CL). We illustrate the interplay of solar and KamLAND data in the left panel of figure 4. The survival probability in KamLAND is given by

$$P_{ee}^{\text{KamL}} \approx \cos^4 \theta_{13} \left(1 - \sin^2 2\theta_{12} \sin^2 \frac{\Delta m_{21}^2 L}{4E} \right), \quad (4)$$

leading to an anti-correlation of $\sin^2 \theta_{13}$ and $\sin^2 \theta_{12}$ [8], see also [14, 34]. In contrast, for solar neutrinos, one has

$$P_{ee}^{\text{solar}} \approx \begin{cases} \cos^4 \theta_{13} \left(1 - \frac{1}{2} \sin^2 2\theta_{12} \right) & \text{low energies,} \\ \cos^4 \theta_{13} \sin^2 \theta_{12} & \text{high energies.} \end{cases} \quad (5)$$

Equation (5) shows a similar anti-correlation as in KamLAND for the vacuum oscillations of low-energy solar neutrinos. For the high-energy part of the spectrum, which undergoes the adiabatic MSW conversion inside the sun and which is subject to the SNO CC/NC measurement, a positive correlation of $\sin^2 \theta_{13}$ and $\sin^2 \theta_{12}$ emerges. As visible from figure 4 (left) and as discussed already in [8, 34], this complementarity leads to a non-trivial constraint on θ_{13} and it allows us to understand the hint for a nonzero value of θ_{13} , which helps us to reconcile the slightly different best fit points for θ_{12} for solar and KamLAND separately [14, 16]. This trend was visible already in pre-SNO-NCD data, though with a significance of

Table 1. Best-fit values with 1σ errors, and 2σ and 3σ intervals (1 d.o.f.) for the three-flavour neutrino oscillation parameters from global data including solar, atmospheric, reactor (KamLAND and CHOOZ) and accelerator (K2K and MINOS) experiments.

Parameter	Best fit	2σ	3σ
Δm_{21}^2 (10^{-5} eV ²)	$7.65^{+0.23}_{-0.20}$	7.25–8.11	7.05–8.34
$ \Delta m_{31}^2 $ (10^{-3} eV ²)	$2.40^{+0.12}_{-0.11}$	2.18–2.64	2.07–2.75
$\sin^2\theta_{12}$	$0.304^{+0.022}_{-0.016}$	0.27–0.35	0.25–0.37
$\sin^2\theta_{23}$	$0.50^{+0.07}_{-0.06}$	0.39–0.63	0.36–0.67
$\sin^2\theta_{13}$	$0.01^{+0.016}_{-0.011}$	≤ 0.040	≤ 0.056

only 0.8σ , see figure 4 (right) showing the present result together with our previous one from v6 of [8].

Let us briefly comment on a possible additional hint for a nonzero θ_{13} from atmospheric neutrino data [15, 30]; the papers [16, 30] by Fogli *et al* find from atmospheric+long-baseline+CHOOZ data a 0.9σ hint for a nonzero value: $\sin^2\theta_{13} = 0.012 \pm 0.013$. In our atmospheric neutrino analysis (neglecting Δm_{21}^2 effects) combined with CHOOZ data, the best fit occurs for $\theta_{13} = 0$ (cf figure 3, right), in agreement with [29]. Also, in the atmospheric neutrino analysis from [31] (which does include Δm_{21}^2 effects, like [16, 30]), the preference for a nonzero θ_{13} is much weaker than the one from [30], with $\Delta\chi^2 \lesssim 0.2$. In our global analysis, the hint from solar+KamLAND gets diluted by the constraint coming from atmospheric+CHOOZ data, and we find the global χ^2 minimum at $\sin^2\theta_{13} = 0.01$, but with $\theta_{13} = 0$ allowed at 0.9σ ($\Delta\chi^2 = 0.87$). Hence, we conclude that at present there is no significant hint for a nonzero θ_{13} . As already stated, the origin of slightly different conclusions of other studies is related to including or neglecting the effect of solar terms in the atmospheric neutrino oscillation analysis, and translates also into a possibly nonmaximal best fit value for θ_{23} . Note however that all analyses agree within $\Delta\chi^2$ values of order 1 and therefore there is no significant disagreement. A critical discussion of the impact of sub-leading effects in atmospheric data on θ_{13} and θ_{23} as well as a comparison of the results of different groups can be found in [33].

Before summarizing, let us update also the determination of the ratio of the two mass-squared differences,

$$\alpha \equiv \frac{\Delta m_{21}^2}{|\Delta m_{31}^2|} = 0.032, \quad 0.027 \leq \alpha \leq 0.038 \quad (3\sigma), \quad (6)$$

which is relevant for the description of CP violation in neutrino oscillations in long-baseline experiments.

4. Summary

In this work, we have provided an update on the status of three-flavour neutrino oscillations, taking into account the latest available world neutrino oscillation data presented at the Neutrino 2008 Conference. Our results are summarized in figures 1–3. Table 1 provides best fit points, 1σ errors and the allowed intervals at 2σ and 3σ for the three-flavour oscillation parameters.

Acknowledgments

This work was supported by MEC grant FPA2005-01269 and by the EC contracts RTN network MRTN-CT-2004-503369 and ILIAS/N6 RII3-CT-2004-506222. We thank Michele Maltoni for collaboration on global fits to neutrino oscillation data.

References

- [1] Robertson H, Decowski P, Gallagher H and Galbiati C 2008 *Neutrino 2008 Conference* Available online at <http://www2.phys.canterbury.ac.nz/~jaa53/>
- [2] Amsler C *et al* 2008 Review of particle physics *Phys. Lett. B* **667** 1
- [3] Schechter J and Valle J W F 1980 Neutrino masses in $SU(2) \times U(1)$ theories *Phys. Rev. D* **22** 2227
Schechter J and Valle J W F 1981 Neutrino masses in $SU(2) \times U(1)$ theories *Phys. Rev. D* **23** 1666
- [4] Bandyopadhyay A *et al* 2007 Physics at a future neutrino factory and super-beam facility arXiv:0710.4947 [hep-ph]
- [5] Nunokawa H, Parke S J and Valle J W F 2008 CP violation and neutrino oscillations *Prog. Part. Nucl. Phys.* **60** 338–402
- [6] Apollonio M *et al* 2003 Search for neutrino oscillations on a long base-line at the CHOOZ nuclear power station *Eur. Phys. J. C* **27** 331–74
- [7] Maltoni M, Schwetz T, Tortola M A and Valle J W F 2003 Status of three-neutrino oscillations after the SNO-salt data *Phys. Rev. D* **68** 113010
- [8] Maltoni M, Schwetz T, Tortola M A and Valle J W F 2004 Status of global fits to neutrino oscillations *New J. Phys.* **6** 122 (arXiv:hep-ph/0405172v6)
- [9] Adamson P *et al* 2008 Measurement of neutrino oscillations with the MINOS detectors in the NuMI beam arXiv:0806.2237 [hep-ex]
- [10] Aharmim B *et al* 2008 An independent measurement of the total active ^8B solar neutrino flux using an array of ^3He proportional counters at the sudbury Neutrino Observatory *Phys. Rev. Lett.* **101** 111301 (arXiv:0806.0989 [nucl-ex])
- [11] Abe S *et al* 2008 Precision measurement of neutrino oscillation parameters with KamLAND *Phys. Rev. Lett.* **100** 221803 (arXiv:0801.4589 [hep-ex])
- [12] The Borexino Collaboration 2008 New results on solar neutrino fluxes from 192 days of Borexino data arXiv:0805.3843 [astro-ph]
- [13] Hahn R L 2008 *Neutrino 2008 Conference* Available online at <http://www2.phys.canterbury.ac.nz/~jaa53/>
- [14] Balantekin A B and Yilmaz D 2008 Contrasting solar and reactor neutrinos with a nonzero value of θ_{13} *J. Phys. G: Nucl. Part. Phys.* **35** 075007 (arXiv:0804.3345)
- [15] Escamilla J, Latimer D C and Ernst D J 2008 Atmospheric neutrino oscillation data constraints on θ_{13} arXiv:0805.2924 [nucl-th]
- [16] Fogli G L, Lisi E, Marrone A, Palazzo A and Rotunno A M 2008 Hints of $\theta_{13} > 0$ from global neutrino data analysis arXiv:0806.2649 [hep-ph]
- [17] Araki T *et al* 2005 Measurement of neutrino oscillation with KamLAND: evidence of spectral distortion *Phys. Rev. Lett.* **94** 081801 (arXiv:hep-ex/0406035)
- [18] Huber P and Schwetz T 2004 Precision spectroscopy with reactor anti-neutrinos *Phys. Rev. D* **70** 053011 (arXiv:hep-ph/0407026)
- [19] Learned J 2008 *Neutrino 2008 Conference* Available online at <http://www2.phys.canterbury.ac.nz/~jaa53/>
- [20] Shimizu I 2007 *TAUP 2007 Conference*
- [21] Aharmim B *et al* 2005 Electron energy spectra, fluxes, and day–night asymmetries of B-8 solar neutrinos from the 391-day salt phase SNO data set *Phys. Rev. C* **72** 055502 (arXiv:nucl-ex/0502021)
- [22] Cleveland B T *et al* 1998 Measurement of the solar electron neutrino flux with the Homestake chlorine detector *Astrophys. J.* **496** 505

- [23] Abdurashitov J N *et al* 2002 Measurement of the solar neutrino capture rate by the Russian–American gallium solar neutrino experiment during one half of the 22-year cycle of solar activity *J. Exp. Theor. Phys.* **95** 181 (arXiv:astro-ph/0204245)
- [24] Altmann M *et al* 2005 Complete results for five years of GNO solar neutrino observations *Phys. Lett. B* **616** 174 (arXiv:hep-ex/0504037)
- [25] Hosaka J *et al* 2006 Solar neutrino measurements in Super-Kamiokande-I *Phys. Rev. D* **73** 112001 (arXiv:hep-ex/0508053)
- [26] Michael D G *et al* 2006 Observation of muon neutrino disappearance with the MINOS detectors and the NuMI neutrino beam *Phys. Rev. Lett.* **97** 191801
- [27] Aliu E *et al* 2005 Evidence for muon neutrino oscillation in an accelerator-based experiment *Phys. Rev. Lett.* **94** 081802
- [28] Ashie Y *et al* 2005 A measurement of atmospheric neutrino oscillation parameters by Super-Kamiokande I *Phys. Rev. D* **71** 112005
- [29] Hosaka J *et al* 2006 Three flavor neutrino oscillation analysis of atmospheric neutrinos in Super-Kamiokande *Phys. Rev. D* **74** 032002 (arXiv:hep-ex/0604011)
- [30] Fogli G L, Lisi E, Marrone A and Palazzo A 2006 Global analysis of three-flavor neutrino masses and mixings *Prog. Part. Nucl. Phys.* **57** 742 (arXiv:hep-ph/0506083)
- [31] Gonzalez-Garcia M C and Maltoni M 2008 Phenomenology with massive neutrinos *Phys. Rep.* **460** 1–129 (arXiv:0704.1800)
- [32] Kajita T 2008 *NuFact05 Conference* Available online at http://www.lnf.infn.it/conference/nufact05/talks2/WG1/Kajita_WG1.ppt
- [33] Schwetz T 2006 Global fits to neutrino oscillation data *Phys. Scr. T* **127** 1 Talk at the *SNOW 2006 Workshop* <http://www.theophys.kth.se/snow2006/060502/01-schwetz.pdf>
- [34] Goswami S and Smirnov A Yu 2005 Solar neutrinos and 1–3 leptonic mixing *Phys. Rev. D* **72** 053011